



## Comparative study on carbon cathodes with and without cobalt phthalocyanine in Li/(SOCl<sub>2</sub> + BrCl) cells

Yong-Sheng Guo<sup>a,b</sup>, Hong-Hua Ge<sup>a,b,\*</sup>, Guo-Ding Zhou<sup>a</sup>, Yi-Ping Wu<sup>a</sup>

<sup>a</sup> Shanghai University of Electric Power, Shanghai Key Laboratory of Colleges and Universities for Corrosion Control in Electric Power System and Applied Electrochemistry, Shanghai 200090, China

<sup>b</sup> Department of Chemical Engineering, School of Environmental and Chemical Engineering, Shanghai University, Shanghai 200444, China

### ARTICLE INFO

#### Article history:

Received 1 March 2009

Received in revised form 30 April 2009

Accepted 8 May 2009

Available online 20 May 2009

#### Keywords:

Cobalt phthalocyanine

Carbon cathode

BCX cell

Li/SOCl<sub>2</sub> cell

### ABSTRACT

The comparative study of carbon cathodes with and without cobalt phthalocyanine (CoPc) in BCX cells (the Li/SOCl<sub>2</sub> cell containing BrCl in the electrolyte) has been carried out by using electrochemical impedance spectroscopy (EIS), constant current discharge curves, scanning electron microscopy (SEM) and X-ray photoelectron spectroscopy (XPS) methods. It is shown that CoPc can improve both the capacity and the voltage of discharge for the BCX cell, and enhance the stability of the open-circuit voltage of the BCX cell. The addition of CoPc to carbon cathode of BCX cells can also decrease the impedance value of the porous carbon cathode, resulting in the considerable decrease of both film resistance and electron transfer resistance. The microstructure and composition of the discharge products on carbon cathodes have been studied using SEM/EDS and XPS analysis.

© 2009 Elsevier B.V. All rights reserved.

## 1. Introduction

Li/SOCl<sub>2</sub> cells have the highest energy density among the realized chemical power sources, high working voltage and stable discharge voltage, and can be used in wide operating temperature ranges and stored for a long time [1–3]. However, the Li/SOCl<sub>2</sub> cell also has some problems such as the safety performance, the voltage delay phenomenon and the large current discharge capabilities [4]. BCX cell refers to the Li/SOCl<sub>2</sub> cell containing BrCl in the electrolyte, which is considered to be the best alternative of the Li/SOCl<sub>2</sub> cell [5–7]. However, there is still a lot of work to do on the study of BCX cell, such as the stability in the process of storage, the improvement of large current delivering capabilities and so on.

Cobalt phthalocyanine (CoPc) is a macrocyclic compound [8], whose structure is shown in Fig. 1. It has been reported that CoPc plays an important role in Li/SOCl<sub>2</sub> cells, which is added to the Li/SOCl<sub>2</sub> cells as electrocatalyst to improve the discharge capacity, the discharge current and the lifespan of the cells [9,10]. The effect of CoPc on the performance of BCX cell was studied in this paper. In order to obtain additional information about the discharge process, the discharge products were analysed using scanning electron microscopy/energy dispersive spectroscopy (SEM/EDS) and XPS.

## 2. Experimental

### 2.1. Preparation of the electrolyte

1 M LiAlCl<sub>4</sub>/SOCl<sub>2</sub> electrolyte was prepared in a three-neck flask, in which LiAlCl<sub>4</sub> and SOCl<sub>2</sub> was refluxed for 10 h in the presence of Li foils in order to remove the impurity and the very small amount of water probably existing in the electrolyte [11,12]. A certain amount of BrCl was added to the electrolyte, then 1 M LiAlCl<sub>4</sub>/SOCl<sub>2</sub> + 2 M BrCl electrolyte was finally made.

### 2.2. Preparation of carbon electrodes

Two types of cathodes were prepared. The CoPc catalysed carbon cathode (cathode A) was made from the mixture of 88% acetylene carbon black (China), 5% CoPc (U.S.A.), 7% diluted PTFE emulsion (60%) and a certain of iso-propyl-alcohol, which were uniformly stirred to turn into a paste. The paste was rolled repeatedly with twin rollers to form a sheet of certain thickness. The sheet was dried at 150 °C for 12 h in an electric vacuum drying oven, and then cut into the cathode. The cathode B was prepared in the same way as above but no CoPc contained.

### 2.3. Experimental cells

Experimental cells were made of PTFE with three-electrode configuration and air-tight. All electrode substrates were made of stainless steel on account of its corrosion resistance, especially

\* Corresponding author. Tel.: +86 21 65700719; fax: +86 21 65700719.  
E-mail address: [gehonghua@shiep.edu.cn](mailto:gehonghua@shiep.edu.cn) (H.-H. Ge).

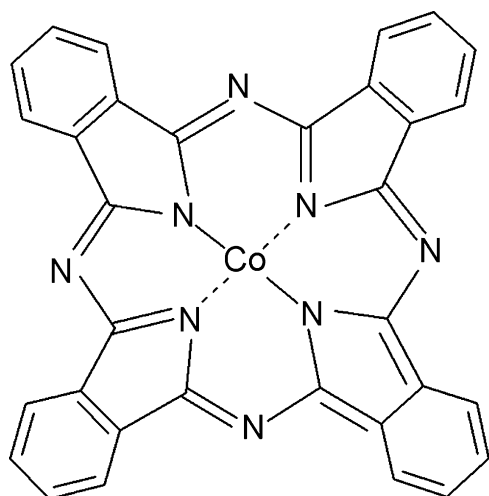


Fig. 1. The structure of cobalt phthalocyanine (CoPc).

pitting resistance against  $\text{SOCl}_2$ . The porous carbon electrodes (cathode A and cathode B) were used as working electrodes with the apparent surface area of  $1.13 \text{ cm}^2$ , and the glass fiber diaphragm was used as a separator. The electrolyte was  $1 \text{ M LiAlCl}_4/\text{SOCl}_2 + 2 \text{ M BrCl}$ , and the reference and auxiliary electrodes were all made of lithium metal.

#### 2.4. Experimental instruments and conditions

The measurement of electrochemical impedance spectroscopy was carried out by using EG&G PARC M283 Potentiostat/Galvanostat, PARC M1025 Frequency Response Analyzer and M398 test software. The range of frequency was  $0.05 \text{ Hz}$  to  $100 \text{ kHz}$  with  $5 \text{ mV}$  of amplitude. The fitting of EIS was done by PAR's 4.51 "Equivalent Circuit" software. The experiment of constant current discharge was performed on a Land battery measurement system and the cut off voltage was  $2 \text{ V}$ . The morphology and EDS of the discharged carbon cathode were obtained using scanning electron microscopy (SEM) on a JEOL field-emission microscope (JSM-6700F).

The carbon cathode was first discharged at constant currents of  $3 \text{ mA}$  for different depths of discharge. After each step of discharge, the carbon cathode was exposed to electrochemical impedance measurement at open-circuit potential (OCP). The cell assembly and all the electrochemical experiments were carried out in the glove box (Braun, Germany) under pure argon atmosphere in which the water was kept below  $0.1 \text{ ppm}$ .

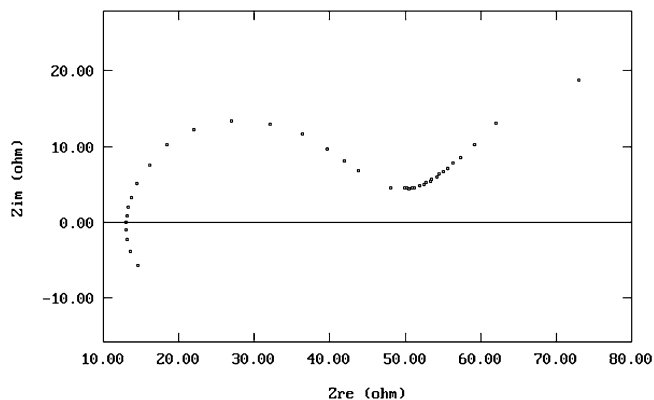


Fig. 2. The Nyquist plot of cathode B in  $\text{LiAlCl}_4/(\text{SOCl}_2 + \text{BrCl})$  solution.

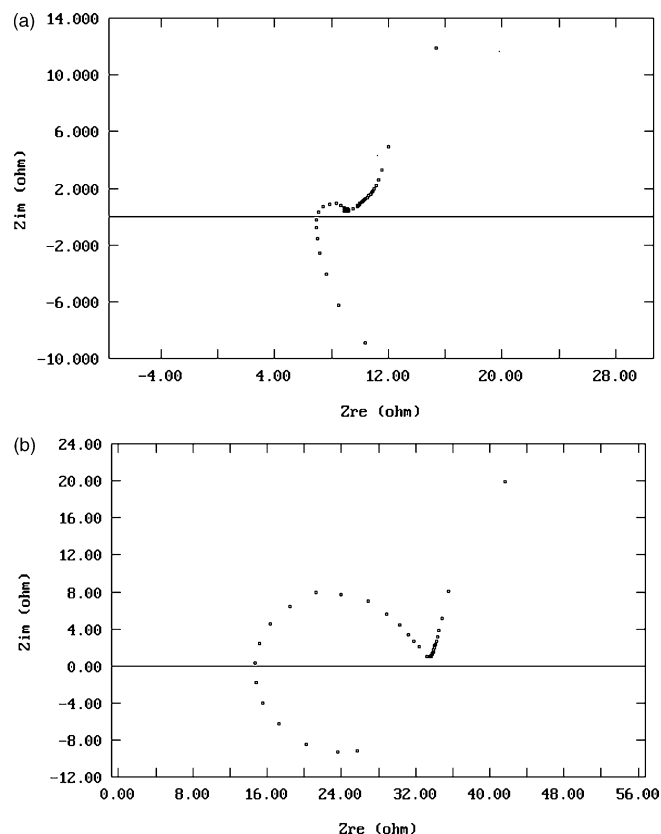


Fig. 3. The Nyquist plots of two carbon cathodes in  $\text{LiAlCl}_4/(\text{SOCl}_2 + \text{BrCl})$  solutions.

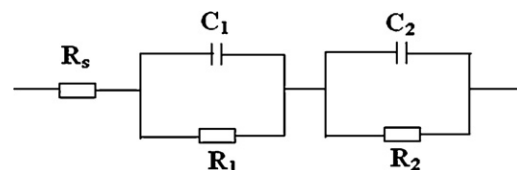


Fig. 4. The equivalent circuit of carbon cathode in  $\text{LiAlCl}_4/(\text{SOCl}_2 + \text{BrCl})$  solution.

### 3. Results and discussion

#### 3.1. The open-circuit voltages vary from time

Table 1 is the comparison of the open-circuit voltages of BCX cells assembled with two carbon electrodes for various storage time. It can be seen that the open-circuit voltage of BCX cell without CoPc decreases slowly with time. The open-circuit voltage of BCX cell with CoPc is  $3.938 \text{ V}$  at the beginning, and increases to  $3.951 \text{ V}$  after a day, and then showed stable. The parallel data show the same tendency. The carbon electrodes with CoPc make the open-circuit voltage stable, which may alleviate the problem that the open-circuit voltage of BCX cell drops during storage.

Table 1

The open-circuit voltages of BCX cells assembled with different carbon cathodes for various storage time.

| The days of storage | 0       | 1       | 3       | 7       | 15      |
|---------------------|---------|---------|---------|---------|---------|
| Cathode B1          | 3.955 V | 3.950 V | 3.946 V | 3.940 V | 3.938 V |
| Cathode B2          | 3.954 V | 3.949 V | 3.943 V | 3.942 V | 3.940 V |
| Cathode A1          | 3.938 V | 3.951 V | 3.952 V | 3.951 V | 3.950 V |
| Cathode A2          | 3.940 V | 3.948 V | 3.951 V | 3.950 V | 3.949 V |

Cathode A1, A2: the carbon cathodes with CoPc; cathode B1, B2: the carbon cathodes without CoPc.

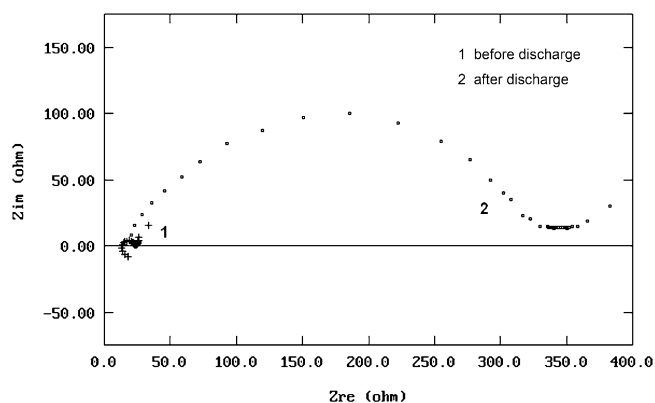


Fig. 5. The Nyquist plots of cathode B in BCX cell before and after discharge at 3 mA.

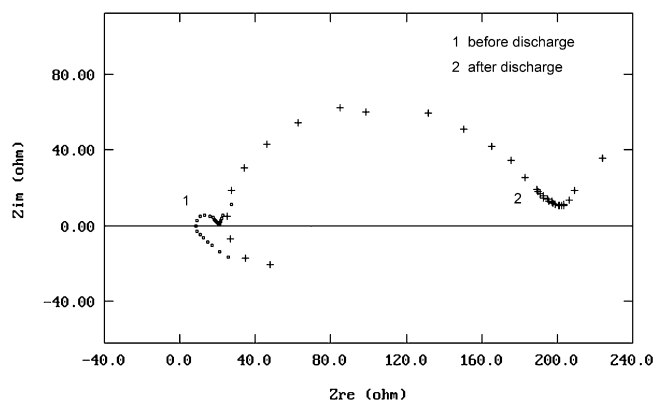


Fig. 6. The Nyquist plots of cathode A in BCX cell before and after discharge at 3 mA.

### 3.2. Electrochemical impedance spectroscopy of carbon cathodes

A typical Nyquist plot of porous carbon electrode is shown in Fig. 2, which includes the high frequency inductive arc, the high frequency capacitive arc and the low frequency capacitive arc [13]. The high frequency inductive arc is somewhat associated with the porosity of the carbon electrode. The high frequency capacitive arc corresponds to the film resistance and the film capacitance of the carbon electrode. The low frequency capacitive arc reflects the  $\text{SOCl}_2$  cathodic reduction process which is carried out at the interface between the electrode surface and the electrolyte.

The Nyquist plots of the two carbon cathodes in electrolyte are presented in Fig. 3 respectively. As the inductive arc at high frequencies has little influence on the discharging characteristics of cells, the impedance spectra in Fig. 3 are mainly composed of two semicircles, so it can be simulated with the equivalent circuit shown in Fig. 4, where  $R_s$  and  $R_1$  represent the solution resistance and the surface film resistance of the porous carbon cathode respectively,  $R_2$  stands for the electron transfer resistance,  $C_1$  represents the film capacitance, and  $C_2$  is the double layer capacitance [14]. The fitting results of Fig. 3 are shown in Table 2.

It has been seen from the fitting results that the impedance values of  $R_1$  and  $R_2$  of cathode A are much smaller than those of cathode B. This illustrates that the addition of CoPc reduces both the surface

**Table 2**  
The fitting results of the experimental data.

| Cathode types | $R_1$ ( $\Omega$ ) | $R_2$ ( $\Omega$ ) |
|---------------|--------------------|--------------------|
| Cathode A     | 1.6856             | 59.394             |
| Cathode B     | 18.754             | 80.11              |

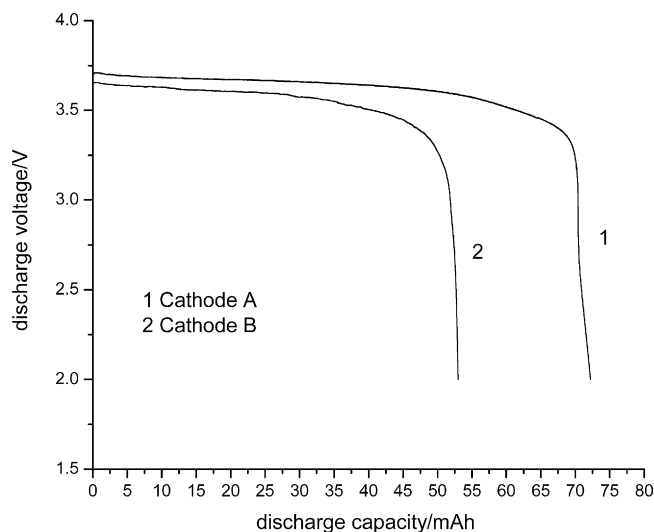


Fig. 7. Constant current discharge curves of BCX cells assembled with two carbon cathodes at 3 mA.

film resistance and the electron transfer resistance at the carbon cathode.

Figs. 5 and 6 are the Nyquist plots of BCX cells assembled with two carbon cathodes before and after the 3 mA discharge. It is seen from the plots that the impedance values of both the cathode A and cathode B increase significantly after discharge (especially the impedance of the high frequency arc), which are attributed to the deposition of LiCl on the surface of the carbon cathodes during discharge.

In some cases there is a straight line in the range of medium frequency in the Nyquist plots. The straight line is attributable to a Warburg impedance that is associated with the diffusion of  $\text{SOCl}_2$  through the LiCl passive film [15]. Comparing Fig. 5 with Fig. 6, it is found that there is straight line in the range of medium-frequency in Fig. 5, and there is no obvious line segment in Fig. 6. It seems that the additive CoPc at the cathode A delays the deposition of LiCl (the discharge product) to some extent or loosens the LiCl passive film, which makes the diffusion of  $\text{SOCl}_2$  going through the LiCl passive film more easily.

The impedance module value at 0.05 Hz ( $|Z|_{0.05}$ ) usually corresponds to the electrode impedance [16]. The larger  $|Z|_{0.05}$  is, the

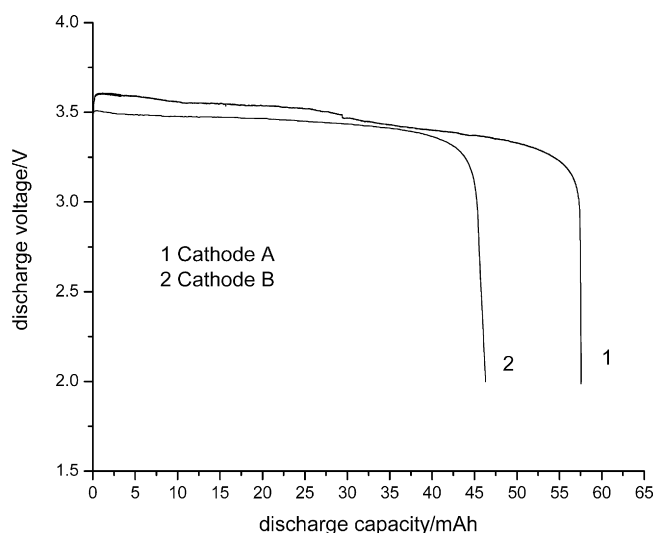
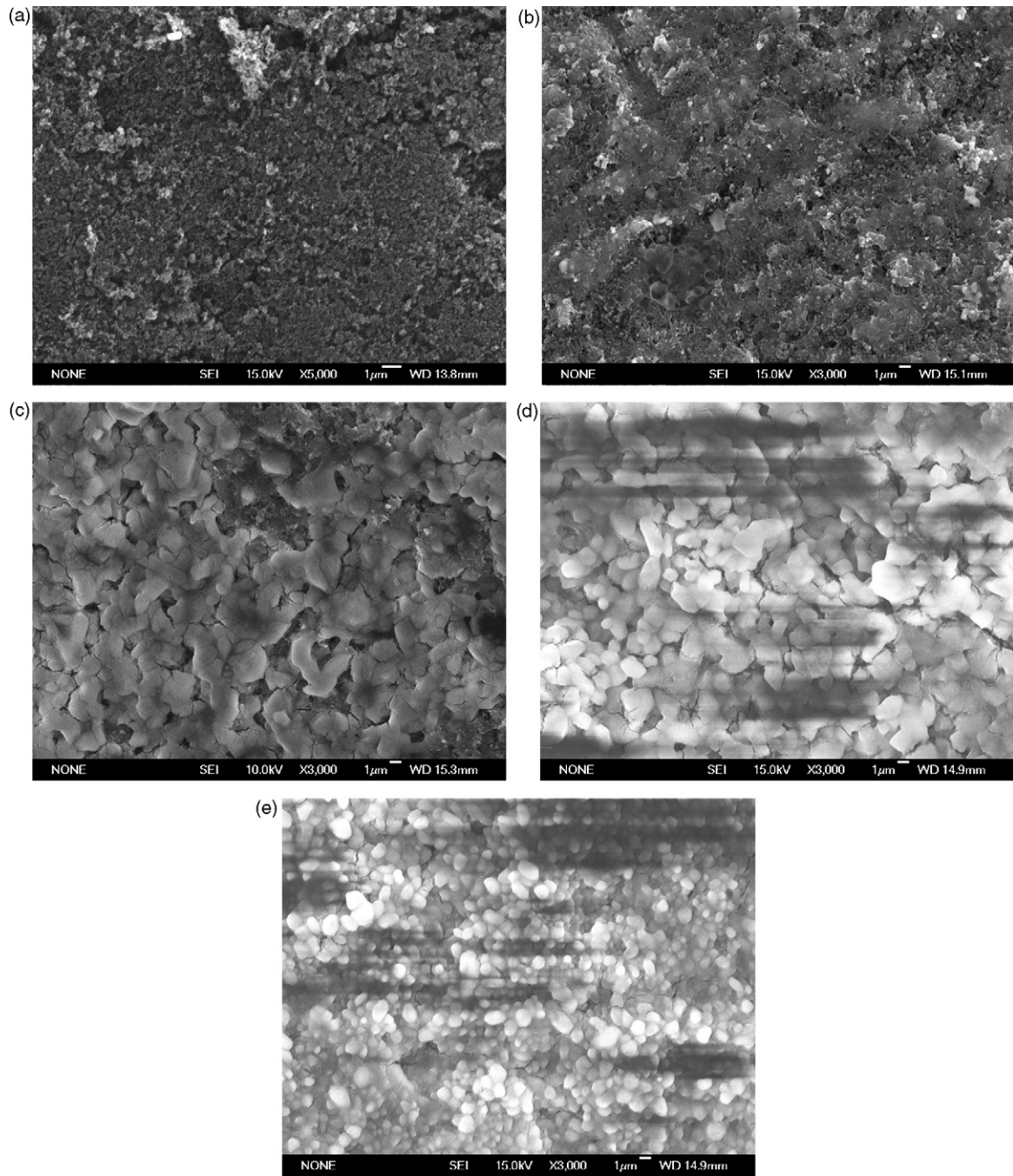


Fig. 8. Constant current discharge curves of BCX cells assembled with two carbon cathodes at 5 mA.



**Fig. 9.** SEM of cathode A in BCX cell for different discharge time at 3 mA. Discharge time: (a) 0 h, (b) 5 h, (c) 10 h, (d) 15 h and (e) 24 h.

bigger the electrode reaction resistance is. Table 3 shows the  $|Z|_{0.05}$  values of the two carbon cathodes in BCX cells before and after discharge. It is indicated from the table that the impedance value of the carbon cathode after discharge increases by one order of magnitude higher than that before discharge. BCX cell in the discharge process produces solid LiCl and others, which deposit on the sur-

face of carbon cathodes. These solid products block the channel of electrode reaction, and decrease greatly the effective action area of carbon cathodes. The electrode impedance value increases significantly, hindering  $\text{SOCl}_2$  reduction on the carbon cathodes. However, interestingly, the impedance values of cathode A before and after discharge are smaller obviously than those of cathode B.

**Table 3**

$|Z|_{0.05}$  values of two cathodes in BCX cells before and after discharge at 3 mA.

| The type of the carbon cathodes | The time of discharge (h) | Cut off voltage (V) | The impedance before discharge ( $\Omega$ ) | The impedance after discharge ( $\Omega$ ) |
|---------------------------------|---------------------------|---------------------|---|--|
| Cathode A                       | 23.5                      | 2                   | 26.92                                       | 226.40                                     |
| Cathode B                       | 16.8                      | 2                   | 37.13                                       | 383.80                                     |



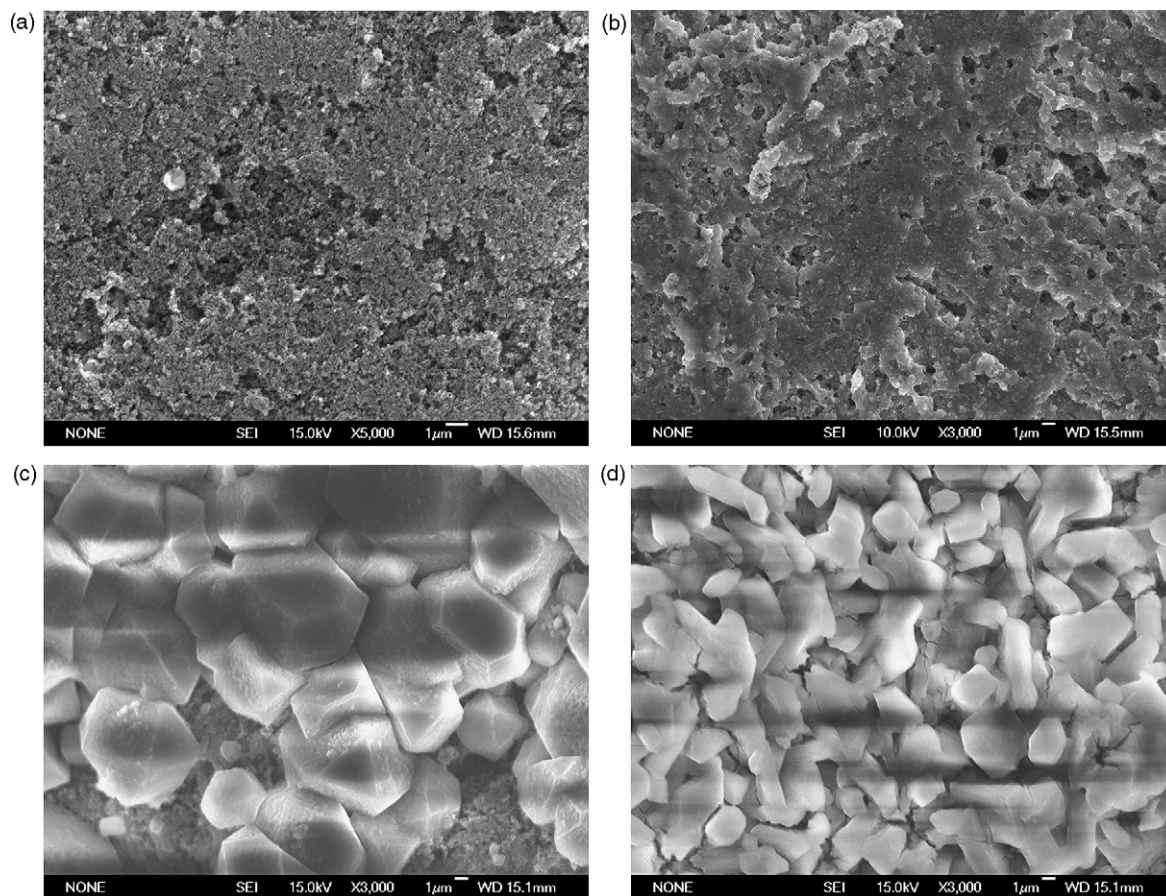


Fig. 10. SEM of cathode B in BCX cell for different discharge time at 3 mA. Discharge time: (a) 0 h, (b) 5 h, (c) 10 h and (d) 17 h

### 3.3. Galvanostatic discharge curves

The constant current discharge curves of BCX cells assembled with two different carbon cathodes are shown in Figs. 7 and 8.

It is shown in Figs. 7 and 8 that the discharge capacity and the discharge voltage of BCX cells assembled with cathode A are higher than those with cathode B.

Table 4 is the comparison of discharge properties of the two cathodes. It shows that under the constant current discharge at 3 mA, the discharge capacity of BCX cell with cathode A is higher by 38.50% than that with cathode B and the average discharge voltage increases by 0.107 V, and under the constant current discharge at 5 mA, the discharge capacity with cathode A is higher by 33.30% than that with cathode B and the average discharge voltage increases by 0.097 V.

### 3.4. Surface analysis of the carbon cathodes

The SEM photographs of cathode A and cathode B after discharge for different time are shown in Figs. 9 and 10 respectively. It is shown that a solid film is formed on the carbon cathode and grows thicker and thicker with discharge time. It is usually considered that the solid films consist of lithium chloride crystallites which cause the passivation of carbon cathode [17].

The solid films of the two types of carbon cathodes after discharge were analysed using XPS. Five kinds of elements Li, Cl, S, O and Al were detected, as shown in Figs. 11–15. The Cl element has a binding energy 199.00 eV, showing its chemical valence  $-1$ . The binding energy of Li element is 56.30 eV and 56.50 eV respectively, showing its chemical valence  $+1$ . The chemical valence of S

is  $+6$  in the form of sulfate, and the simple substance of S was not detected in the discharge products, illustrating that the chemical state of product of S in the discharge process had been changed as a result of the addition of BrCl and CoPc. The simple substance S, which commonly exists as cathode reduction product in Li/SOCl<sub>2</sub> cell [10], changed into the form of sulfate. Al element does not exist in the form of simple substance, but in halide form, such as AlCl<sub>3</sub>

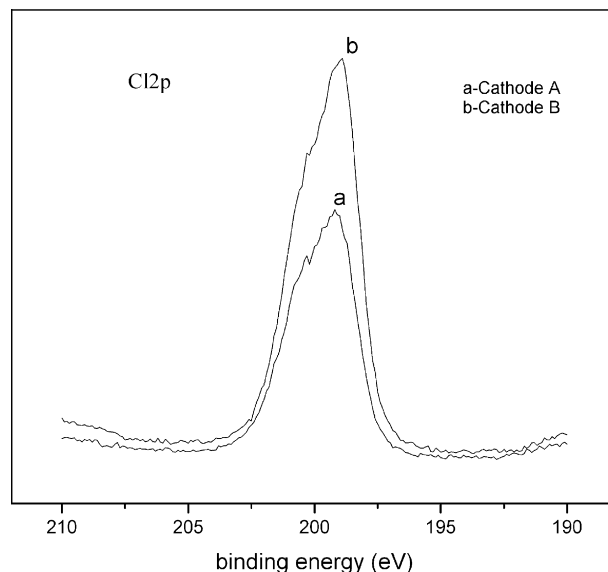
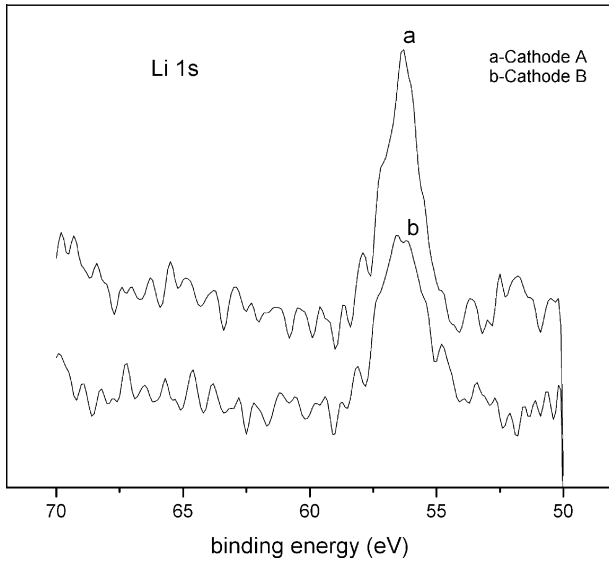


Fig. 11. Cl element XPS spectra of sediments on two cathodes.

**Table 4**  
Discharge data of BCX cells with two cathodes.

| The type of carbon cathode | The discharge current (mA) | The discharge capacity (mAh) | The average voltage (V) | The discharge time (h) |
|----------------------------|----------------------------|------------------------------|-------------------------|------------------------|
| Cathode A                  | 3                          | 72.20                        | 3.6408                  | 24.06                  |
| Cathode B                  | 3                          | 52.13                        | 3.5335                  | 17.37                  |
| Cathode A                  | 5                          | 57.72                        | 3.5872                  | 11.54                  |
| Cathode B                  | 5                          | 43.30                        | 3.4903                  | 8.66                   |



**Fig. 12.** Li element XPS spectra of sediments on two cathodes.

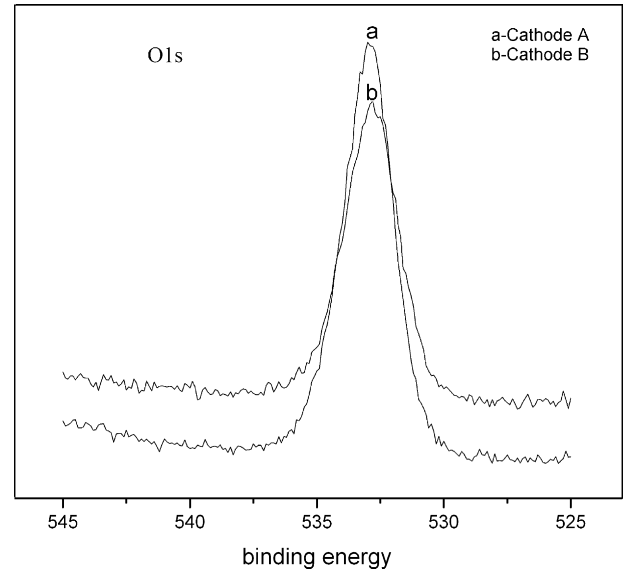


**Fig. 14.** O element XPS spectra of sediment on two cathodes.

which may decompose from the electrolyte  $\text{LiAlCl}_4$ . Cl and Li are the main elements of the films. EDS analysis indicates that the content of chloride is above 90%. It is believed that the main components of the carbon cathode discharge products are the insoluble solid LiCl.

SEM/EDS and XPS studies on the microstructure and composition of discharge products show there is no essential difference in composition between cathode A and cathode B. However, it is of interest from the comparison of the shape of the crystals on the surface of cathode, as shown in Fig. 9d, e and Fig. 10c, d that in

the case of cathode A, the size of LiCl crystals is much smaller and the shape is irregular, which makes the LiCl passive film loose [18], and for cathode B LiCl crystals of regular shape prevails and the size of LiCl crystals is much larger. This result is in accordance with that from electrochemical impedance measurements. Therefore, it is concluded that the discharge mechanism taking place on the cathode surface is similar for both cathode types. The observed differences in cathodic behavior should be attributed to the addition of CoPc.

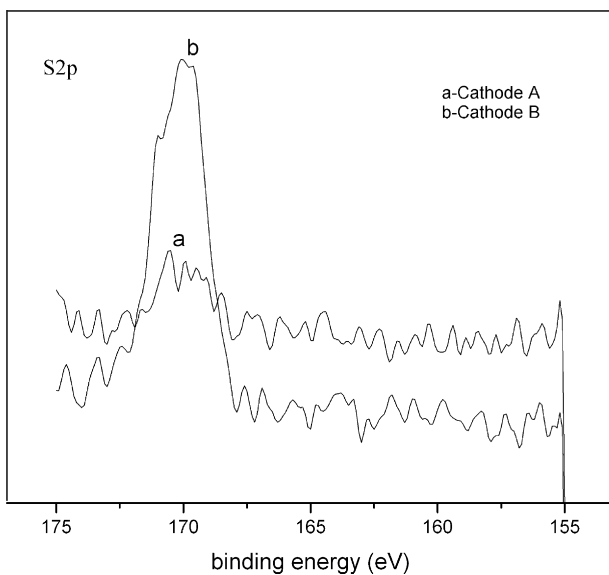


**Fig. 13.** S element XPS spectra of sediments on two cathodes.

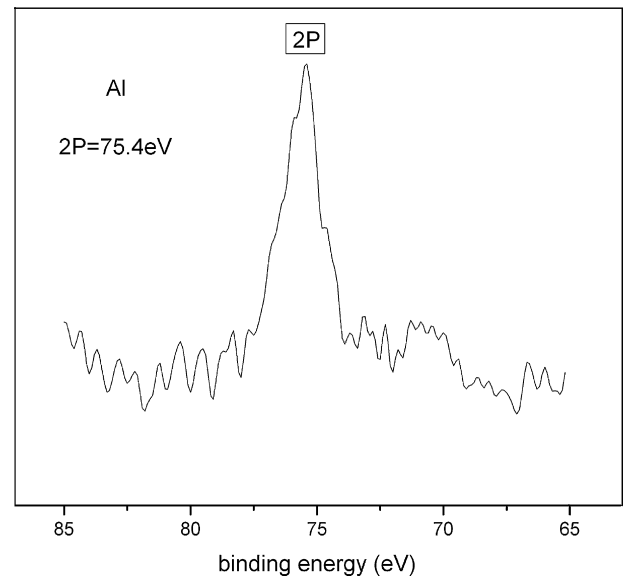


**Fig. 15.** Al element XPS spectra of sediment on cathode A.

#### 4. Conclusions

CoPc as the electrocatalyst added to the carbon cathode improves both the discharge voltage and the capacity of BCX cells, and makes the open-circuit voltage of BCX cells much more stable.

It is found from the measurements of electrochemical impedance spectroscopy for both cathode A and cathode B that the surface film resistance  $R_1$  and the electron transfer resistance  $R_2$  of cathode A are much smaller than those of cathode B, and the addition of CoPc decreases the reaction resistance of cathode reduction and increases the discharge capacity of cathode. The additive CoPc benefits to the diffusion of  $\text{SOCl}_2$  through the passive film of cathode.

SEM measurements exhibit that a solid film forms on the carbon cathode and grows thicker and thicker with discharge time. XPS analysis of the solid films of cathode A and cathode B after discharge indicates that Cl and Li are main elements of the films and have chemical valence  $-1$  and  $+1$  respectively. The content of chloride in discharge products is above 90%. The chemical valence of S is  $+6$  in the form of sulfate, and the simple substance of S is not detected. SEM/EDS and XPS studies of the microstructure and composition of discharge products show that there is no essential difference in composition between cathode A and cathode B, but exists difference in the shape and the size of LiCl crystals. In the case of cathode A the size of LiCl crystals is small and the shape is irregular.

#### Acknowledgements

Support of this study by Shanghai Leading Academic Discipline Project (Project Number: p1304), Science and Technology Commission of Shanghai (Project Numbers: 06DZ22010 and 061612043) are gratefully acknowledged.

#### References

- [1] R.M. Spotnitz, G.S. Yeduvaka, G. Nagasubramanian, *J. Power Sources* 163 (2006) 578.
- [2] C. Menachem, H. Yamin, *J. Power Sources* 136 (2004) 268.
- [3] Y.S. Guo, H.H. Ge, G.D. Zhou, Y.P. Wu, *Battery Bimonthly* 38 (1) (2008) 408.
- [4] M. Gaberšček, S. Pejovnik, *J. Electrochem. Soc.* 146 (3) (1999) 933.
- [5] K.M. Abraham, M. Alamgir, S.T. Perrotti, *J. Electrochem. Soc.* 135 (11) (1988) 2686.
- [6] C.C. Liang, P.W. Krehl, *J. Appl. Electrochem.* 11 (1981) 563.
- [7] P.W. Krehl, C.C. Liang, *J. Electrochem. Soc.* 130 (13) (1983) 451.
- [8] J.L. Huang, Y.R. Peng, N.S.H. Chen, *Spectrosc. Spectral Anal.* 21 (1) (2001) 1–6.
- [9] K.M. Abraham, M. Alamgir, E.B. Willstaedt, et al., *Electrochim. Acta* 37 (3) (1992) 531–543.
- [10] K.M. Abraham, M. Alamgir, W.P. Killroy, *J. Power Sources* 26 (3–4) (1989) 597–602.
- [11] H.H. Ge, G.D. Zhou, Y.P. Wu, J. Liu, *Battery Bimonthly* 35 (6) (2005) 420–421.
- [12] H.H. Ge, Y.S. Guo, Y.P. Wu, et al., *J. Appl. Electrochem.* 39 (2009) 155–158.
- [13] C.H. Kim, Su-II Pyun., *J. Electrochem. Soc.* 150 (9) (2003) A1176–A1181.
- [14] Y.L. Zhang, C.S. Cha, *Electrochim. Acta* 37 (7) (1992) 1207.
- [15] S.B. Lee, S. Pyun, E.J. Lee, *Electrochim. Acta* 47 (2001) 855–864.
- [16] G.D. Zhou, *Bull. Electrochem.* 2 (7) (1991) 60–65.
- [17] M. Jakič, K. Gaberšček, *Electrochim. Acta* 40 (17) (1995) 2723.
- [18] P.A. Bernstein, A.B.P. Lever, *Inorg. Chem.* 34 (1995) 933–937.